Erastin sensitizes glioblastoma cells to temozolomide by restraining xCT and cystathionine-γ-lyase function

LIANGYU CHEN[1], XINXING LI[1], LIBO LIU[2,3], BO YU[1], YIXUE XUE[2,3] and YUNHUI LIU[1]

[1]Department of Neurosurgery, Shengjing Hospital of China Medical University;
[2]Department of Neurobiology, College of Basic Medicine, China Medical University;
[3]Institute of Pathology and Pathophysiology, China Medical University, Shenyang, Liaoning, P.R. China

Abstract. Glioblastoma multiforme (GBM) is one of the most common encephalic malignant tumors. Due to a high recurrence rate and a lack of effective treatments, the average survival rate remains low. Temozolomide (TMZ), a class of alkylating agent, is widely used as a first-line therapeutic drug during the adjuvant treatment for GBM patients. However, most patients exhibit a palpable resistance to TMZ treatment. Additionally, the underlying mechanism remains to be clarified. In this study, glutathione (GSH) and reactive oxygen species (ROS) levels were found to be closely associated with the sensitivity of GBM cells to TMZ. We also found that TMZ markedly induced xCT, the subunit of glutamate/cystine transporter system x_c^- expression, which together with the GSH synthesis was increased while the TMZ-inducible ROS level was decreased in GBM cells. In addition, the cystathionine γ-lyase (CTH) acivity, a key enzyme in the transsulfuration pathway was enhanced by TMZ, which insured a cysteine supply and GSH synthesis in a compensatory manner when xCT was blocked. Thus, the individual inhibition of xCT by siRNA and a pharmacological inhibitor (sulfasalazine) only partially inhibited GSH synthesis and moderately enhanced the GBM cell sensitivity to TMZ. However, the TMZ-induced cytotoxicity was markedly increased along with a marked decrease in GSH levels as result of co-treatment with erastin, which inhibited cysteine uptake from xCT transporter and suppressed CTH activity, leading to impaired transformation from methionine to cysteine. In conclusion, to GBM therapy with a drug combination of TMZ and erastin may be beneficial.

Introduction

Glioblastoma multiforme (GBM) is one of the most common gliomas, and is extremely lethal in all central nervous system tumors (1). GBM infiltrates into normal brain tissues where a tumor and the normal brain tissue have no clear demarcation, due to glioma cells having a high mobility and possessing strong invasive properties (2,3). Thus, it is difficult to completely remove the tumor through surgical resection. Additionally, GBM has been proven to resist radio- and chemotherapy (4). Although patients undergo the most aggressive regimens of debulking surgeries, radiotherapy together with adjuvant chemotherapy results in a median survival of ~14 months (5). At present, there are no effective methods to prevent a relapse of the tumor by residual neoplastic cells following surgery and radiotherapy.

Temozolomide (TMZ) is a class of alkylating agent approved by the Food and Drug Administration (FDA). TMZ is widely used as a standard-of-care during clinical treatment. However, it only results in a slight increase of overall survival of GBM patients. Furthermore, most patients are resistant to TMZ in the clinic (6). O^6-methylguanine produced by DNA methyl transferase mainly mediates the cytotoxicity of TMZ and triggers cell cycle-dependent DNA damage, ensuring cell death. Thus, O^6-methylguanine-DNA methyl transferase (MGMT) limits the therapeutic effect of TMZ by removing O^6-methylguanine (7,8). However, findings of previous GBM cell line studies showed that the activity of MGMT was not entirely consistent with the resistance of GBM to TMZ, i.e., even in MGMT-silenced GBM cells, the effect of TMZ was limited (8). The exact cell death pathway induced by TMZ and the molecular mechanisms affecting the efficacy of TMZ in GBM cells remain to be determined.

The glutamate/cystine antiporter system x_c^- is an obligate sodium-independent amino acid antiporter, comprising 12-pass transmembrane transporter protein xCT (SLC7A11) which is connected to the 4F2 cell surface antigen 4F2hc

(CD98/SLC3A2) by a disulfide bridge (9,10). System x_c^- transports extracellular cystine into cells in exchange for intracellular glutamate at a ratio of 1:1, and maintaining intracellular cysteine pools is important (10). Cysteine is a crucial material in glutathione (GSH) synthesis, which is indispensable for maintaining intracellular redox balance and drug metabolism (11,12). xCT expression is mediated by the oxidative stress-response transcription factor NF-E2 related to factor 2 (Nrf2) and activation of transcription factor 4 (ATF4) (13). xCT is expressed in many types of malignancies and is associated with tumor growth and metastasis. It is also associated with resistance to chemotherapy and poor survival (13-17). Accordingly, xCT has been considered as a potential therapeutic target (13,14,16,17). Sulfasalazine (SASP) is a sulfa drug used for inflammatory bowel diseases and rheumatoid arthritis treatment and is a widely recognized xCT-specific inhibitor (18). Although it has been suggested that the inhibitory effect of SASP on xCT can suppress GBM cell growth, the combination of SASP combined with TMZ for GBM treatment in the clinic has yielded controversial results (19,20). Erastin (ERA) is a voltage-dependent anion channels (VDAC)-binding small molecule that is selectively lethal to some cancer cells (21). Compared to SASP, ERA exerts a stronger inhibitory effect on xCT (22). In addition, ERA is able to inhibit the activity of certain GSH-related enzymes, such as glutathione peroxidase 4 (GPx4), resulting in more lethal oxidative damage to cells (23). ERA can cause a unique form of cell death on iron-dependent tumor cells as compared to conventional apoptosis, necrosis and autophagy (22).

In many types of cells cysteine is derived from an imported xCT process, however, there is also a transsulfuration pathway in which methionine is transferred to cysteine via catalysis by cystathionine β-synthase (CSE) and cystathionine-γ-lyase (CTH) (24,25). In brain carcinoma cells such as glioma cells and astrocytes, most cysteine originates from the reduction process of cystine imported by xCT under normal conditions. However, when xCT is blocked or GSH is decreased, the transsulfuration pathway is activated, which insures the cysteine supply for GSH synthesis in a compensatory manner (26,27). Furthermore, CTH activity may limit cysteine synthesis via the methionine transsulfuration pathway (28,29). However, whether transsulfuration and CTH are involved in TMZ resistance remains to be elucidated.

In this study, we demonstrated that GBM cells were sensitive to TMZ with a downregulation of the GSH level. TMZ enhanced xCT expression in an Nrf2- and ATF4-dependent manner. Moreover, it activated the transsulfuration pathway in GBM cells by enhancing CTH activity. Erastin restrained xCT and CTH resulting in a marked increase of TMZ cytotoxicity, which may be beneficial to GBM therapy.

Materials and methods

Materials. Temozolomide (TMZ, 3, 4-dihydro-3-methyl-4-oxoimidazo [5, 1-d]-1, 2, 3, 5-tetrazine-8-carboxamide), deferoxamine mesylate (DFO), erastin (ERA), *N*-Acetyl-L-cysteine (NAC), sulfasalazine (SASP), propargylglycine (PPG), as well as Dulbecco's modified Eagle's medium (DMEM) and bovine serum albumin (BSA) were obtained from Sigma-Aldrich (St. Louis, MO, USA). Dimethylsulfoxide (DMSO) was obtained from Wako Pure Chemical (Osaka, Japan). CellROX Orange reagent was purchased from Life Technologies (Tokyo, Japan). Anti-xCT antibody (ab37185) was obtained from Abcam (Cambridge, MA, USA). Anti-Nrf2 antibody (sc-722), anti-ATF4 antibody (sc-200) and anti-LaminB antibody (sc-56144) were purchased from Santa Cruz Biotechnology, Inc. (Dallas, TX, USA).

Cell culture. The human A172, U87-MG and T98G malignant glioblastoma multiforme cells were purchased from the American Tissue Culture Collection (Rockville, MD, USA). GBM-N6 and GBM-N15, isolated from a grade IV human glioblastoma, were a generous gift from Dr Dongcheng Wang at Shandong University.

The cells were maintained in DMEM containing 10% fetal bovine serum (Gibco, Grand Island, NY, USA) with 100 U/ml penicillin and 100 μg/ml streptomycin (Gibco). The cells were cultured at 37˚C with 5% CO_2 and saturated humidity.

Cloning of CTH cDNA and stable transfection. The overexpression vector of CTH was constructed by using the primer 5'-CGT CCC AGC ATG CAG AAG AA-3' and 5'-CAG TTA TTC AGA AGG TCT GGC CC-3'. The constructs containing CTH cDNA were then subcloned into the pIRES2-EGFP expression vector (Clontech) as previously reported (30). For stable transfection, GBM-N15 cells were transfected with linearized constructs by using FuGENE transfection reagent (Roche Applied Science) according to the manufacturer's instructions. After 48 h of transfection, the cells were seeded in 35-mm dish at a density of $5x10^4$ cells/dish. The following day, the culture media was refreshed containing 500 μg/ml G418 (Life Technologies) for antibiotic selection. After five weeks of culturing the selected antibiotics, survival-transfected cells were collected. Stable-transfected cells were used within 15 passages as previously reported (30).

Determination of intracellular reactive oxygen species (ROS). U87, T98G and GBM-N15 cells were plated in 12-well plates at a density of $5.0x10^5$ cells/well and cultured overnight. The cells were treated with DMSO or 400 μM TMZ for 3 h. In the experiment in which TMZ and ERA or SASP were used as co-treatment methods, $5.0x10^5$ cells/well of GBM-N15 cells were plated in 12-well plates. After 24 h, the culture medium was refreshed with 400 μM TMZ and 5 μM ERA or 0.3 mM SASP. After 3-h incubation, the culture medium was replaced with fresh culture medium containing 5 μM CellRox Orange Reagent, and the cells were incubated at 37˚C for an additional 30 min. After washing with PBS twice, the Tali Image-based Cytometer (Life Technologies) was used to detect the stained cells.

RNA preparation and RT-qPCR. Total RNA from GBM-N15 cells was isolated by using TRIzol reagent (Life Technologies, Carlsbad, CA, USA) according to the manufacturer's instructions. cDNAs were synthesized using the Transcriptor First Strand cDNA Synthesis kit (Roche, Shanghai, China). The quantitative RT-PCR analyses were performed using SYBR Premix Ex Taq II (Takara Bio) and the CFX Real-time PCR Detection System (Bio-Rad, Hercules, CA, USA). The primers used for RT-qPCR were: human *xCT*, forward: 5'-CCA TGA

ACG GTG GTG TGT T-3' and reverse: 5'-GAC CCT CTC GAG ACG CAA C-3'); human *Nrf2*, forward: 5'-ACT CCC AGG TTG CCC AC-3' and reverse: 5'-GTA GCC GAA GAA ACC TCA TTG TC -3'); human *ATF4*, forward: 5'-TGA AGG AGT TCG ACT TGG ATG CC-3' and reverse: 5'-CAG AAG GTC ATC TGG CAT GGT TTC-3'); human *CTH*, forward: 5'-GCC CAG TTC CGT GAA TCT AA-3' and reverse: 5'-CAT GCT GAA GAG TGC CCT TA-3'); and human *Cyclophilin A*, forward: 5'-ATG CTG GAC CCA ACA CAA AT-3' and reverse 5'-TCT TTC ACT TTG CCA AAC ACC-3'). *Cyclophilin A* was used as an internal control.

Protein extraction and immunoblot analysis. The cells were washed three times with PBS, lysed by using the buffer of 20 mM Tris-HCl (pH 7.5), 150 mM NaCl, 1% Triton X-100, 1 mM EDTA, and sonicated to shear the DNA. Protein concentrations were determined using the bicinchoninic acid assay kit (Pierce, Rockford, IL, USA) according to the manufacturer's instructions. 2-Mercaptoethanol (1%) and bromophenolblue (0.01%) were added into each sample. Protein (10 μg) per lane was separated by SDS-PAGE and then transferred onto PVDF membranes (Millipore, Billerica, MA, USA). The membranes were blocked with 5% BSA-PBS with 0.1% Tween-20 (PBST). For protein visualization, the membranes were blotted with primary antibodies against Nrf2, ATF4, xCT and LaminB. Peroxidase-conjugated anti-rabbit IgG was applied as the secondary antibody. Protein bands were detected using ImmunoStar chemiluminescent reagent (Wako Pure Chemical).

siRNA transfection. After 24 h of seeding in 6-well plates, GBM-N15 cells were transfected with siRNA by using Lipofectamine RNAiMAX (Life Technologies). Human CTH siRNA (sc-78973), human xCT siRNA (sc-76933), human Nrf2 (sc-37030) and control siRNA (sc-37007) were purchased from Santa Cruz Biotechnology, Inc.; and human ATF4 siRNA was synthesized as the following sequence: forward: 5'-GCC UAG GUC UCU UAG AUG ATT-3' and reverse: 5'-UCA UCU AAG AGA CCU AGG CTT-3'. After another 24 h of incubation, the transfected cells were treated with TMZ for the indicated times. Subsequently, immunoblot analysis, cell viability determination and intracellular GSH detection were performed.

Cell viability analysis. Cell viability was evaluated by using the Cell Counting kit-8 (DojinDo, Kumamoto, Japan) according to the manufacturer's instructions. Briefly, A172, U87, T98G, GBM-N6 and GBM-N15 cells were plated in 96-well plates at a density of 5.0x10^4 cells/well. On the following day, the cells were treated with TMZ of a concentration from 50 to 800 μM. After 48 h of incubation, the cell viability was detected. For the TMZ-inducible cell death in xCT knockdown GBM-N15 cells experiment, the cells were transfected with control or xCT siRNA as described above. After 24 h of transfection, the cells were seeded in 96-well plates at a density of 5.0x10^4 cells/well and incubated overnight. The following day, 50-600 μM TMZ were added to the transfected cells and incubated for an additional 48 h. In TMZ and SASP (or ERA) co-treatment experiments, the GBM-N15 cells were seeded in 96-well plates at a density of 5.0x10^4 cells/well. After 24 h, the culture media were replaced with the media containing increased

doses of TMZ in the presence and absence of 0.3 mM SASP or 5 μM ERA. After 48 h, the cell viability was analyzed. For the experiment in which desferrioxamine (DFO) decreased ERA-processed TMZ cytotoxicity, the cells were seeded as described above. The following day, the medium was replaced with 50 or 100 μM TMZ and 5 μM ERA in the presence or absence of 100 μM DFO.

Intracellular cysteine and GSH analysis. U87, T98G and GBM-N15 cells were plated in 6-well plates at a density of 6.0x10^5 cells/well and cultured overnight. The following day, DMSO or 400 μM TMZ was introduced for a 24-h incubation. For the TMZ-induced GSH levels experiment, xCT was knocked down with siRNA as described above. The following day, the cells were incubated in the presence or absence of 400 μM TMZ. After 24 h, the cells were subjected to GSH analysis. For the TMZ and SASP (or ERA) co-treatment experiment, the GBM-N15 cells were plated in 6-well plates as described above. The following day, 400 μM TMZ with 0.3 mM SASP or 5 μM ERA were added into the medium, and the cells were incubated for 24 h. To determine amino acid deprivation, the cells were plated as mentioned above. The following day, the culture medium was replaced with a certain amino acid deprivation culture medium (methionine, cystine or cystathionine) as shown in Fig. 5A. Following incubation for 30 min at 37°C, 400 μM TMZ was introduced. After 24 h of treatment, intracellular cysteine and GSH levels were measured as previously described (31).

Determination of CTH activity. GBM-N15 cells were plated on 6-well plates at a density of 5.0x10^5 cells/well. After 24 h, the medium was refreshed with SASP, ERA or PPG. After 30-min incubation at 37°C, 400 μM TMZ was introduced for the next 24-h treatment. Subsequently, intracellular CTH activity was determined as previously described (27).

Statistical analysis. Data were presented as the means ± SEM of at least three independent experiments. One-way ANOVA with the Bonferroni post-hoc test was used to determine significant differences between the means. The difference between the means was considered significant at p<0.05.

Results

ROS and GSH levels are closely associates with the sensitivity of GBM cells to TMZ treatment. To determine GBM cell line sensitivity to TMZ, we identified three frequently used GBM cell lines in the laboratory: A172, U87 and T98G cells. GBM-N6 and GBM-N15GBM cell lines were also identified in glioma patients in stage IV. As shown in Fig. 1A, U87 and A172 cells were moderately sensitive to TMZ; however, T98G, GBM-N6 and GBM-N15 cells were significantly resistant to TMZ. The three cell lines were screened and U87, T98G and GBM-N15 cells were used to detect constitutive and TMZ-inducible ROS levels. The ROS level in U87 cells was significantly increased by TMZ treatment, while there were no significant changes for the ROS level in T98G and GBM-N15 cells (Fig. 1B). Correspondingly, the GSH level was only slightly enhanced by TMZ treatment in U87 cells, but was much more significantly elevated in T98G
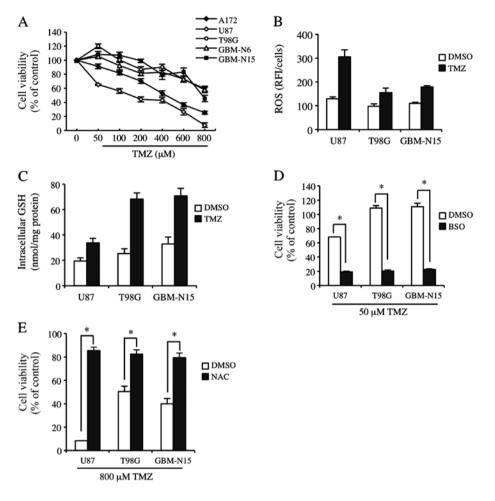
Figure 1. Intracellular GSH and ROS levels are associated with TMZ inducible cytotoxicity to different GBM cell lines. (A) A172, U87, T98G, GBM-N6, and GBM-N15 cells were treated with TMZ in a series of concentrations as indicated for 48 h. The cell viability was assessed by using CCK-8. (B) The cells were subjected to 400 μM TMZ treatment for 3 h, and then ROS levels were detected. (C) After 40 μM TMZ was treated for 24 h, intercellular GSH was determined. (D and E) The cells were co-treated with 50 μM TMZ with 0.5 mM BSO (D) or 800 μM TMZ with 1 mM NAC (E). After 48 h of incubation, the cell viability was measured using CCK-8. Data are presented as means ± SEM from three independent experiments, *p<0.05.

and GBM-N15 cells, suggesting that the cells with a low GSH level and consequently a high ROS level were sensitive to TMZ (Fig. 1C). To confirm the association between resistance to TMZ and the GSH level in the cells, buthione sulfoximine (BSO), an inhibitor in GSH synthesis, was introduced in the experiment. The results showed that BSO almost completely abrogated the resistance of GBM cells to TMZ (Fig. 1D). We also analyzed the effect of NAC on TMZ-inducible cytotoxicity, which is an antioxidant and functions as a source of cysteine and GSH (32). As shown in Fig. 1E, NAC abolished the cytotoxicity of TMZ to GBM cells. These results indicated that the intracellular ROS and GSH levels are closely associated with the resistance of GBM cells to TMZ treatment.

TMZ markedly induced xCT expression in GBM-N15 cells. Results of previous studies indicated that GSH and ROS levels were associated with xCT expression. Moreover, the pharmacologic inhibitor for xCT enhanced the cytotoxicity of TMZ (13,16,20,33). To examine the contribution of xCT to resistance to TMZ, we detected TMZ-inducible xCT expression. The RT-qPCR results showed that 50, 100, 200, 400 and 800 μM TMZ increased *xCT* mRNA expression by 2.5-, 3.6-, 4.8-, 7.6- and 8.1-fold, respectively (Fig. 2A), and the induced

xCT mRNA expression increased significantly from 6 to 24 h (Fig. 2B). Consistent with this result, the xCT protein level was also increased significantly by TMZ treatment (Fig. 2D). To identifiy the stability of *xCT* mRNA induced by TMZ, 0.5 μg/ml of actinomycin D was used to sever the gene transcription. As shown in Fig. 2C, TMZ did not change the stability of *xCT* mRNA significantly. These observations suggested that TMZ markedly induced the expression of xCT at transcription level.

TMZ induces xCT expression via Nrf2 and ATF4 activation pathway. Nrf2 and ATF4 are involved in the regulation of xCT expression in human bladder carcinoma cells (13). To investigate the contribution to the expression of Nrf2 and ATF4 in TMZ-inducible xCT, Nrf2 and ATF4 expression levels were detected in GBM-N15 cells. The results showed that 400 μM TMZ markedly induced the expression of Nrf2 and ATF4 at mRNA and protein levels, and the inductions peaked from 6 to 12 h (Fig. 3A and B). As shown in Fig. 3C, the constitutive- and TMZ-triggered expression of *xCT* mRNA was decreased in Nrf2 and ATF4 knockdown cells. In addition, TMZ-inducible Nrf2 and ATF4 protein expression was decreased individually by siRNA targeting Nrf2 and ATF4 (Fig. 3D and E).
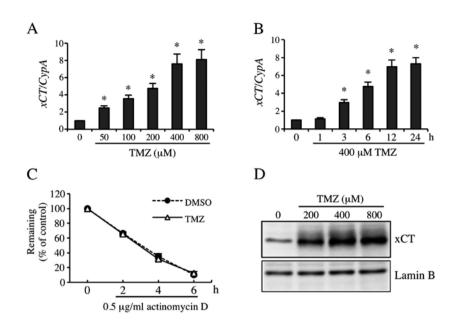
Figure 2. TMZ induces xCT expression in GBM-N15 cells. (A) The cells were treated with 50-800 μM TMZ for 12 h, and then *xCT* mRNA was determined by RT-qPCR. *CypA* was used as an internal control. (B) GBM-N15 cells were exposed to 400 μM TMZ for 1-24 h. *xCT* mRNA was evaluated by RT-qPCR. Data are presented as means ± SEM. *p<0.05. (C) The cells were co-treated with 400 μM TMZ and 0.5 μg/ml actinomycin D for 2-6 h. Data are presented as a fold of 0 h control. (D) TMZ induced xCT protein expression was detected by using immonoblot analysis.
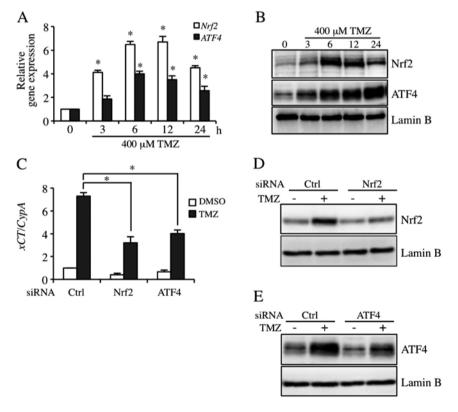

Figure 3. TMZ upregulates xCT in an Nrf2- and ATF4-dependent manner. (A and B) GBM-N15 cells were exposed to 400 μM TMZ for 3-24 h, then Nrf2 and ATF4 mRNA and protein levels were evaluated by (A) RT-qPCR and (B) immunoblot analysis. (C) GBM-N15 cells were transfected with Nrf2 or ATF4 siRNA as described in Materials and methods. After 24 h of incubation, the cells were treated with 400 μM TMZ for 6 h and then subjected to RT-qPCR for xCT mRNA determination. (D and E) The knockdown effect of Nrf2 and ATF4 siRNAs was confirmed by immunoblot analysis. Data are presented as means ± SEM, *p<0.05.

xCT inhibition significantly sensitizes GBM-N15 cells to TMZ. In order to study the role of xCT in the resistance to TMZ, we inhibited the function of xCT by applying xCT siRNA or pharmacologic xCT inhibitors. We confirmed that transfection with xCT siRNA effectively reduced constitutive and TMZ-inducible xCT expression (Fig. 4B). Fig. 4A shows that the sensitivity of GBM cells to TMZ was significantly increased in the xCT knockdown GBM-N15 cells. The
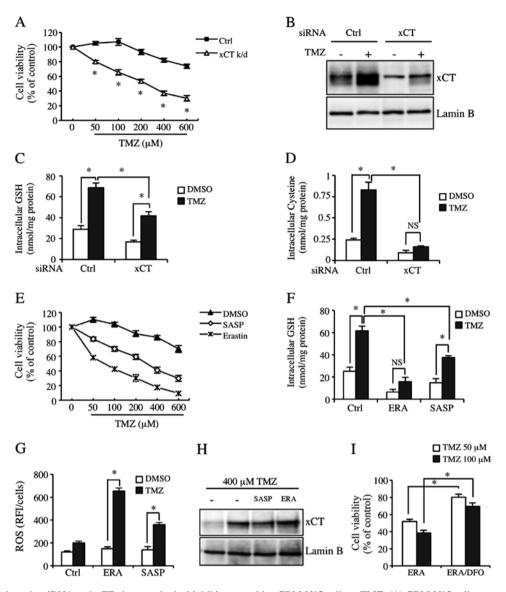
Figure 4. xCT knockdown by siRNA and xCT pharmacological inhibitors sensitize GBM-N15 cells to TMZ. (A) GBM-N15 cells were transfected with xCT or control siRNA. The cells were subjected to 50-600 μM TMZ treatment for 48 h. The cell viability was assessed as previously described. (B) Immunoblot analysis of xCT siRNA-transfected GBM-N15 cells. (C and D) GBM-N15 cells were transfected with xCT or control siRNA. After 24 h, the cells were processed with 400 μM TMZ for another 24 h. Intracellular GSH (C) and cysteine (D) assessments were subsequently performed. (E) GBM-N15 cells were co-treated with an increasing concentration of TMZ as indicated combined with 0.3 mM SASP or 0.5 μM ERA for 48 h. The cell viability was detected by CCK-8 as above. Intracellular GSH (F) and ROS (G) were measured in 400 μM TMZ in the presence of SASP- or ERA-treated GBM-N15 cells. (H) xCT expression was assessed by immunoblotting. (I) GBM-N15 cells were treated as indicated for 48 h and then subjected to cell viability analysis. Data are presented as means ± SEM. *$p < 0.05$; NS, not significant.

cytotoxicity of TMZ was also increased at a physiological concentration (50 μM) (Fig. 4A). Since xCT was crucial for maintaining cysteine pool and GSH synthesis in cells, we detected intracellular cysteine and GSH levels. The results showed that the basic level and TMZ-inducible cysteine level in xCT knockdown cells was decreased significantly (Fig. 4D). Although the TMZ-inducible GSH level was inhibited by the effect of xCT knockdown, the cysteine level was not significantly reduced as compared to the control group (Fig. 4C). In addition, we used the pharmacologic inhibitors of xCT, SASP and ERA to block the properties of xCT in another experiment. Similarly, SASP and ERA significantly decreased the TMZ-inducible GSH level and the resistance to TMZ (Fig. 4E and F). However, the regulation of ERA on TMZ-inducible cytotoxicity and intracellular GSH level

in the cells was much stronger than the regulation of xCT siRNA and SASP, and it almost completely abolished the increase of TMZ-inducible GSH level (Fig. 4E and F, middle lane). Consistent with this result, SASP and ERA enhanced the TMZ-inducible ROS level in GBM-N15 cells, with the effect of ERA being much more significant than that of SASP (Fig. 4G). Additionally, SASP and ERA did not affect TMZ-inducible xCT expression (Fig. 4H). Additionally, the increase of sensitivity to TMZ by applied ERA was partially eliminated by an Fe (III) chelator known as desferrioxamine (DFO) (Fig. 4I). These data indicated TMZ-induced cell death partially resulted from oxidative stress. The TMZ-inducible xCT upregulation increased the cysteine and GSH levels in GBM-N15 cells, which inhibited oxidative stress and reduced the effect of TMZ.
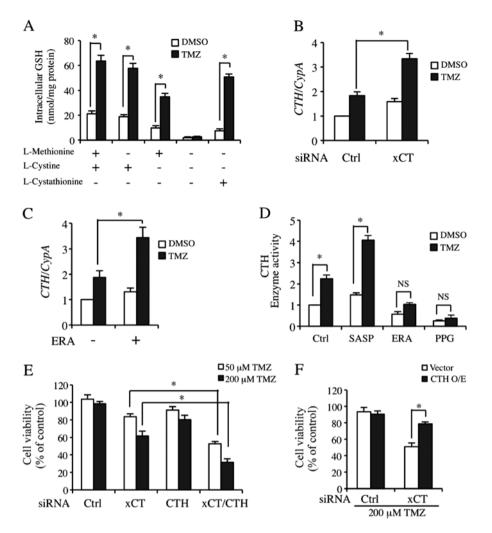
Figure 5. CTH participates in GSH synthesis in TMZ-treated GBM-N15 cells. (A) GBM-N15 cells were cultured in amino acid-deprived medium as indicated for 24 h. Intercellular GSH evaluation was performed. (B) TMZ-inducible CTH mRNA was analyzed in xCT knockdown cells. (C) TMZ (400 μM) in combination with 0.5 μM ERA-activated CTH mRNA was measured. (D) CTH enzyme activity was detected in the cells treated as indicated. (E) xCT and CTH were knocked down individually or simultaneously in GBM-N15 cells and exposed to 50 or 200 μM TMZ for 48 h. The cell viability was measured as before. (F) The CTH overexpression stable cells were transfected with control or xCT siRNA and exposed to 200 μM TMZ for 48 h. Then cell viability was detected. Data are presented as means ± SEM, *p<0.05; NS, not significant.

Transsulfuration pathway supports the necessary cysteine for GSH synthesis as a compensatory pathway when xCT expression was inhibited. Fig. 4C and D shows that although the cysteine level was markedly decreased, GSH synthesis was only partly affected. Kandil *et al* stated that cystathionine-γ-lyase (CTH), the key regulatory enzyme in transsulfuration pathway is activated to maintain GSH synthesis when xCT was blocked (34). We found that the TMZ-inducible GSH level was only partially downregulated due to cysteine deprivation in the media (Fig. 5A). However, GSH level was markedly decreased in the basic and TMZ-processed cells when methionine and cysteine were deprived (Fig. 5A, lane 3). Moreover, cystathionine almost completely acquired the role of methionine and cysteine (Fig. 5A, lane 5). We then detected *CTH* mRNA regulation by TMZ treatment in the cells transfected with ctrl or xCT siRNA. As shown in Fig. 5B, TMZ significantly upregulated the expression of *CTH* mRNA in xCT knockdown cells. *CTH* expression was also increased slightly in xCT-silenced cells without TMZ treatment in a compensatory manner (Fig. 5B). In another experiment, we detected

the effect of TMZ on *CTH* expression and its enzyme activities when xCT was inhibited by pharmacological inhibitors. Of note, CTH enzyme activity that was processed by TMZ and SASP co-treatment was markedly increased (Fig. 5D, Lane 2). By contrast, ERA almost completely abolished the increase of TMZ-inducible CTH enzyme activity (Fig. 5D, Lane 3). PPG as an inhibitor to the transsulfuration pathway was the positive control (Fig. 5D, Lane 4). We also found that ERA did not decrease the basic and TMZ-inducible *CTH* mRNA expression (Fig. 5C). In order to clarify that CTH was involved in the resistance to TMZ in GBM-N15 cells, we applied siRNA transfection targeting xCT and CTH independently or in combination. CTH knockdown alone was not able to decrease resistance to TMZ. However, when CTH and xCT were knocked down simultaneously, TMZ-inducible cytotoxicity was significantly increased under either a physiological (50 μM) or a high (200 μM) concentration of TMZ (Fig. 5E). Similarly, the overexpression of CTH suppressed the increase of TMZ-triggered cytotoxicity in xCT knockdown cells (Fig. 5F).
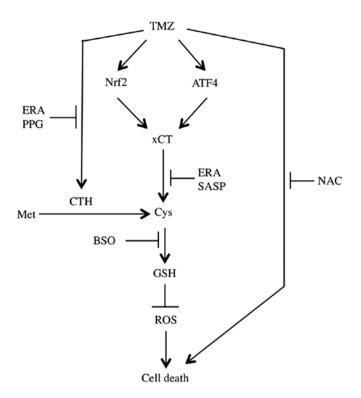
Figure 6. Hypothetic model for TMZ-induced xCT and CTH activation and their contributions to TMZ resistance of GBM cells.

Discussion

In clinical therapy for GBM patients, new combined treatments and drugs are currently under the Phase 1 or 2 clinic trials (35,36); however, TMZ as a first-line treatment is indispensable. Wide resistance to TMZ affects its application, and the mechanism of resistance remain to be elucidated (6-8). Therefore, elucidation of the mechanism involved in the resistance to TMZ is crucial for improving the effect as an anticancer drug. Previous studies have reported that the cytotoxicity of TMZ was mainly mediated by O^6-methylguanine, and a satisfactory result of TMZ treatment required functional DNA mismatch repair (MMR) and low MGMT levels as preconditions (37,38). However, recent studies have found that resistance to TMZ was associated with various factors. For instance, miR-128 and miR-149 regulate the invasion and chemosensitivity of GBM cells to TMZ by targeting Rap1B-mediated cytoskeletal and associated molecular alterations (39). Another example is Galectin-1 (Gal1) which regulates resistance to TMZ by targeting the unfolded protein response to endoplasmic reticulum stress (ERS). Moreover, the cell protective autophagy has been reported to contribute to TMZ-induced cell death (40). The production of ROS and the disruption of AKT/mTOR signal have been demonstrated to contribute to the TMZ resistance (41). In this study, we focused on the contribution of TMZ-inducible ROS upregulation and the maintainable cysteine pool and GSH synthesis by xCT transporting and transsulfuration pathway in the resistance to TMZ (Fig. 6).

xCT as a transporter is closely associated with GSH synthesis and ROS accumulation. Additionally, xCT is a potential target of cancer treatment (13,16). In many different types of tumors, pharmacological inhibition of xCT function by SASP exerts an inhibitory effect on tumor cell growth, and decreases the invasion of tumors, such as lymphoma, hepatocellular carcinoma, prostate cancer, bladder carcinoma and, glioma (13,16,34,42,43). Furthermore, it has been proven that the effect of chemo- and radiotherapy may be improved with inhibition on the function of xCT. xCT is an independent predictive factor of poor prognosis and associated with tumor invasion in GBM patients. The findings in the present study coincide with the results of Ye *et al* (13), xCT is strongly induced by TMZ in an Nrf2- and ATF4-dependent manner.

Following the knockdown by xCT siRNA or pharmacological inhibition by SASP and ERA, the ROS level increased while the GSH synthesis level decreased. This process regulates the sensitivity of GBM cells to TMZ treatment. Consequently, xCT is an important factor in the resistance of GBM cells to TMZ. However, the cysteine level in the cells decreased significantly when xCT was knocked down by siRNA, although a marked reduction in the GSH level was not observed. A similar result was confirmed in the co-processing experiment by SASP and TMZ. We found that when we deprived methionine and cysteine in media independently or together, methionine was important to GSH synthesis when cysteine was deprived.

Additionally, cystathionine almost completely replaced cysteine and methionine. These results suggest that another GSH synthesis pathway besides that of xCT exists, such as the transsulfuration pathway. TMZ strongly induces the expression of CTH mRNA and enhances the related enzyme activity, which is critical in the transsulfuration pathway, especially when xCT is inhibited. TMZ has been found to significantly induce the expression of Nrf2 and ATF4. Nrf2 and ATF4 have been found to increase GSH production via multiple mechanisms (44). However, loss of ATF4 impairs GSH production by inhibiting the expression of CTH (45). However, the relevance between TMZ-induced increase of Nrf2 and ATF4 expression and the CTH enzyme regulation, and whether TMZ induced other related enzymes such as CBS (cystathionine β-synthase) in the transsulfuration pathway for GSH synthesis remain to be clarified and the experiments confirmed.

SASP as an xCT pharmacological inhibitor is a class of sulfa drugs that is approved by the Food and Drug Administration (FDA). SASP has been applied to Chron disease therapy in the clinic for a long time. ERA as small molecular compounds is another xCT pharmacological inhibitor that has been recently identified (22). Although the two inhibitors can effectively block cysteine uptake as well as GSH synthesis, there are other synthesis pathways besides xCT, the GSH synthesis has no absolute reliability on xCT. ERA significantly inhibits CTH activity and affects synthesis resulting from the xCT and transsulfuration pathways, thus the effect of TMZ is significantly elevated. However, ERA is limited with regard to the amelioration of TMZ cytotoxicity by applied SASP, because a low cysteine level in cells enables CTH activity with a co-processing treatment by SASP and TMZ. This may be one reason for the controversy regarding whether SASP has a therapeutic effect for GBM. Of note, the cell death caused by applying TMZ and ERA together may be partially rescued by DFO. This type of cell death is to some

degree an Fe (III)-dependent process, described as ferroptosis in a recent study (22). ERA highly preferentially selected to injure RAS-mutant tumors (22). In the present study, the results did not show that there is a RAS-mutant in GBM cells. However, the continuously activated RAS was involved in the dialog between tumor and immune system (46). ERA was involved in the regulation of ferroptotic cancer cell death by inhibiting the activity of GPx4 (glutathione peroxidase 4) (23). Moreover, GPx4 is highly associated with tumor growth, and is a significant risk factor for breast cancer when GPx4 is continuously activated (47,48). However, whether ERA ameliorated GBM cell resistance to TMZ by inhibiting GPx4 activity and increasing the injury of oxidative stress for cells requires further investigation.

The present study shows that TMZ-inducible xCT upregulation and CTH activation were involved in the resistance of GBM cells to TMZ. In addition, ERA was able to block xCT and reduce CTH activity simultaneously. As a result, the cytotoxicity of TMZ was significantly increased. The combined treatment of TMZ and ERA may therefore greatly benefit GBM therapy.

Acknowledgements

References

1. Friedman HS, Kerby T and Calvert H: Temozolomide and treatment of malignant glioma. Clin Cancer Res 6: 2585-2597, 2000.
2. Gunther W, Pawlak E, Damasceno R, Arnold H and Terzis AJ: Temozolomide induces apoptosis and senescence in glioma cells cultured as multicellular spheroids. Br J Cancer 88: 463-469, 2003.
3. Knauth M, Wirtz CR, Tronnier VM, Aras N, Kunze S and Sartor K: Intraoperative MR imaging increases the extent of tumor resection in patients with high-grade gliomas. AJNR Am J Neuroradiol 20: 1642-1646, 1999.
4. Nakada M, Nakada S, Demuth T, Tran NL, Hoelzinger DB and Berens ME: Molecular targets of glioma invasion. Cell Mol Life Sci 64: 458-478, 2007.
5. Stupp R, Mason WP, van den Bent MJ, et al: Radiotherapy plus concomitant and adjuvant temozolomide for glioblastoma. N Engl J Med 352: 987-996, 2005.
6. Burnet NG, Jefferies SJ, Benson RJ, Hunt DP and Treasure FP: Years of life lost (YLL) from cancer is an important measure of population burden - and should be considered when allocating research funds. Br J Cancer 92: 241-245, 2005.
7. Bocangel DB, Finkelstein S, Schold SC, Bhakat KK, Mitra S and Kokkinakis DM: Multifaceted resistance of gliomas to temozolomide. Clin Cancer Res 8: 2725-2734, 2002.
8. Hegi ME, Diserens A, Gorlia T, et al: MGMT gene silencing and benefit from temozolomide in glioblastoma. New Engl J Med 352: 997-1003, 2005.
9. Conrad M and Sato H: The oxidative stress-inducible cystine/glutamate antiporter, system x (c) (-): cystine supplier and beyond. Amino Acids 42: 231-246, 2012.
10. Sato H, Tamba M, Ishii T and Bannai S: Cloning and expression of a plasma membrane cystine/glutamate exchange transporter composed of two distinct proteins. J Biol Chem 274: 11455-11458, 1999.
11. Okuno S, Sato H, Kuriyama-Matsumura K, et al: Role of cystine transport in intracellular glutathione level and cisplatin resistance in human ovarian cancer cell lines. Br J Cancer 88: 951-956, 2003.
12. Lu SC: Glutathione synthesis. Biochim Biophys Acta 1830: 3143-3153, 2013.
13. Ye P, Mimura J, Okada T, et al: Nrf2- and ATF4-dependent up-regulation of xCT modulates the sensitivity of T24 bladder carcinoma cells to proteasome inhibition. Mol Cell Biol 34: 3421-3434, 2014.
14. Toyoda M, Kaira K, Ohshima Y, et al: Prognostic significance of amino-acid transporter expression (LAT1, ASCT2, and xCT) in surgically resected tongue cancer. Br J Cancer 110: 2506-2513, 2014.
15. Yoshikawa M, Tsuchihashi K, Ishimoto T, et al: xCT inhibition depletes CD44v-expressing tumor cells that are resistant to EGFR-targeted therapy in head and neck squamous cell carcinoma. Cancer Res 73: 1855-1866, 2013.
16. Guo W, Zhao Y, Zhang Z, et al: Disruption of xCT inhibits cell growth via the ROS/autophagy pathway in hepatocellular carcinoma. Cancer Lett 312: 55-61, 2011.
17. Chen RS, Song YM, Zhou ZY, et al: Disruption of xCT inhibits cancer cell metastasis via the caveolin-1/beta-catenin pathway. Oncogene 28: 599-609, 2009.
18. Gout PW, Buckley AR, Simms CR and Bruchovsky N: Sulfasalazine, a potent suppressor of lymphoma growth by inhibition of the x(c)- cystine transporter: a new action for an old drug. Leukemia 15: 1633-1640, 2001.
19. Robe PA, Martin DH, Nguyen-Khac MT, et al: Early termination of ISRCTN45828668, a phase 1/2 prospective, randomized study of sulfasalazine for the treatment of progressing malignant gliomas in adults. BMC Cancer 9: 372, 2009.
20. Takeuchi S, Wada K, Nagatani K, Otani N, Osada H and Nawashiro H: Sulfasalazine and temozolomide with radiation therapy for newly diagnosed glioblastoma. Neurol India 62: 42-47, 2014.
21. Yagoda N, von Rechenberg M, Zaganjor E, et al: RAS-RAF-MEK-dependent oxidative cell death involving voltage-dependent anion channels. Nature 447: 864-868, 2007.
22. Dixon SJ, Lemberg KM, Lamprecht MR, et al: Ferroptosis: an iron-dependent form of nonapoptotic cell death. Cell 149: 1060-1072.
23. Yang WS, SriRamaratnam R, Welsch ME, et al: Regulation of ferroptotic cancer cell death by GPX4. Cell 156: 317-331, 2014.
24. Giordana L, Mantilla BS, Santana M, Silber AM and Nowicki C: Cystathionine γ-lyase, an enzyme related to the reverse transsulfuration pathway, is functional in Leishmania spp. J Eukaryot Microbiol 61: 204-213, 2014.
25. Romero I, Téllez J, Yamanaka LE, Steindel M, Romanha AJ and Grisard EC: Transsulfuration is an active pathway for cysteine biosynthesis in Trypanosoma rangeli. Parasit Vectors 7: 197, 2014.
26. McBean GJ: The transsulfuration pathway: a source of cysteine for glutathione in astrocytes. Amino Acids 42: 199-205, 2012.
27. Manna P and Jain SK: Vitamin D up-regulates glucose transporter 4 (GLUT4) translocation and glucose utilization mediated by cystathionine-gamma-lyase (CSE) activation and H2S formation in 3T3L1 adipocytes. J Biol Chem 287: 42324-42332, 2012.
28. Rao AM, Drake MR and Stipanuk MH: Role of the transsulfuration pathway and of gamma-cystathionase activity in the formation of cysteine and sulfate from methionine in rat hepatocytes. J Nutr 120: 837-845, 1990.
29. Liu G, Casqueiro J, Bañuelos O, Cardoza RE, Gutiérrez S and Martín JF: Targeted inactivation of the mecB gene, encoding cystathionine-gamma-lyase, shows that the reverse transsulfuration pathway is required for high-level cephalosporin biosynthesis in Acremonium chrysogenum C10 but not for methionine induction of the cephalosporin genes. J Bacteriol 183: 1765-1772, 2001.
30. Yang G, Cao K, Wu L and Wang R: Cystathionine gamma-lyase overexpression inhibits cell proliferation via a H2S-dependent modulation of ERK1/2 phosphorylation and p21Cip/WAK-1. J Biol Chem 279: 49199-49205, 2004.
31. Sasaki H, Sato H, Kuriyama-Matsumura K, et al: Electrophile response element-mediated induction of the cystine/glutamate exchange transporter gene expression. J Biol Chem 277: 44765-44771, 2002.
32. Wu G, Fang YZ, Yang S, Lupton JR and Turner ND: Glutathione metabolism and its implications for health. J Nutr 134: 489-492, 2004.
33. Chung WJ and Sontheimer H: Sulfasalazine inhibits the growth of primary brain tumors independent of nuclear factor-kappaB. J Neurochem 110: 182-193, 2009.
34. Kandil S, Brennan L and McBean GJ: Glutathione depletion causes a JNK and p38MAPK-mediated increase in expression of cystathionine-gamma-lyase and upregulation of the transsulfuration pathway in C6 glioma cells. Neurochem Int 56: 611-619, 2010.

35. Hottinger AF, Aissa AB, Espeli V, *et al*: Phase I study of sorafenib combined with radiation therapy and temozolomide as first-line treatment of high-grade glioma. Br J Cancer 110: 2655-2661, 2014.
36. Bartels U, Wolff J, Gore L, *et al*: Phase 2 study of safety and efficacy of nimotuzumab in pediatric patients with progressive diffuse intrinsic pontine glioma. Neuro Oncol 16: 1554-1559, 2014.
37. Margison GP and Santibanez-Koref MF: O6-alkylguanine-DNA alkyltransferase: role in carcinogenesis and chemotherapy. Bioessays 24: 255-266, 2002.
38. Zhang J, Stevens MF and Bradshaw TD: Temozolomide: mechanisms of action, repair and resistance. Curr Mol Pharmacol 5: 102-114, 2012.
39. She X, Yu Z, Cui Y, *et al*: miR-128 and miR-149 enhance the chemosensitivity of temozolomide by Rap1B-mediated cytoskeletal remodeling in glioblastoma. Oncol Rep 32: 957-964, 2014.
40. Lin CJ, Lee CC, Shih YL, *et al*: Resveratrol enhances the therapeutic effect of temozolomide against malignant glioma in vitro and in vivo by inhibiting autophagy. Free Radic Biol Med 52: 377-391, 2012.
41. Yin H, Zhou Y, Wen C, *et al*: Curcumin sensitizes glioblastoma to temozolomide by simultaneously generating ROS and disrupting AKT/mTOR signaling. Oncol Rep 32: 1610-1616, 2014.
42. Dai L, Cao Y, Chen Y, Parsons C and Qin Z: Targeting xCT, a cystine-glutamate transporter induces apoptosis and tumor regression for KSHV/HIV-associated lymphoma. J Hematol Oncol 7: 30, 2014.
43. Doxsee DW, Gout PW, Kurita T, *et al*: Sulfasalazine-induced cystine starvation: potential use for prostate cancer therapy. Prostate 67: 162-171, 2007.
44. Ehren JL and Maher P: Concurrent regulation of the transcription factors Nrf2 and ATF4 mediates the enhancement of glutathione levels by the flavonoid fisetin. Biochem Pharmacol 85: 1816-1826, 2013.
45. Dickhout JG, Carlisle RE, Jerome DE, *et al*: Integrated stress response modulates cellular redox state via induction of cystathionine gamma-lyase: cross-talk between integrated stress response and thiol metabolism. J Biol Chem 287: 7603-7614, 2012.
46. Yang BC, Wang YS, Liu HS and Lin SJ: Ras signaling is involved in the expression of Fas-L in glioma. Lab Invest 80: 529-537, 2000.
47. Bermano G, Smyth E, Goua M, Heys SD and Wahle KW: Impaired expression of glutathione peroxidase-4 gene in peripheral blood mononuclear cells: a biomarker of increased breast cancer risk. Cancer Biomark 7: 39-46, 2010.
48. Schneider M, Wortmann M, Mandal PK, *et al*: Absence of Absence of glutathione peroxidase 4 affects tumor angiogenesis through increased 12/15-lipoxygenase activity. Neoplasia 12: 254-263, 2010.